



Measurements of the ambient dose equivalent rates around the Manyoni uranium deposit in Tanzania

Lolila^{a*}, F.; Mazunga^a, M.S.

^a Department of Physics, University of Dar es Salaam, P.O. Box 35063, Dar es Salaam, Tanzania
faridalolila855@gmail.com

ABSTRACT

In this study, pre-mining ambient gamma dose equivalent rates at 1 m above the ground were measured using a Gamma-Scout portable radiation survey meter at two sites, A and B, around the Manyoni uranium deposit in Tanzania. Site A is expected to receive mine-dust particles with an aerodynamic diameter $\leq 10 \mu\text{m}$ (PM₁₀) that have mean annual ground level concentrations (AGLC) $\geq 10\%$ of the WHO air quality guideline limit of $20 \mu\text{g}/\text{m}^3$, and Site B is expected to receive PM₁₀ with a mean AGLC $\geq 20 \mu\text{g}/\text{m}^3$. At Site A, the average of the ambient dose equivalent rates was $0.25 \pm 0.03 \mu\text{Sv}/\text{h}$ and ranged from 0.08 to $0.69 \mu\text{Sv}/\text{h}$. Similarly, at Site B, the average of the ambient dose equivalent rates was $0.23 \pm 0.02 \mu\text{Sv}/\text{h}$ and ranged from 0.12 to $0.34 \mu\text{Sv}/\text{h}$. The effect of the local geology on the measured dose rates was also presented. Since the ambient dose equivalent is an operational quantity for area monitoring, the results of this study will be very useful for comparing with the operational monitoring results of Sites A and B once uranium mining starts in Manyoni. This can help mine operators and regulatory agencies keep an eye on any rise in background radiation so they can take the necessary measures to safeguard locals and the environment from the harmful effects of ionising radiation.

Keywords: background radiation, ambient dose equivalent rate, uranium deposit.



1. INTRODUCTION

Natural background radiation is and has always been a part of our environment. It consists primarily of high-energy cosmic ray particles that collide with the earth's atmosphere and radioactive nuclides that originated in the earth's crust and are present everywhere, including in the human body [1]. The potential for uranium mining to increase levels of background radiation has prompted many researchers to determine background radiation levels in the areas surrounding uranium mines and deposits [2–7]. In the areas surrounding the Manyoni uranium deposit, there is a concern that future uranium mining may contaminate the environment if not carefully regulated. As a result, pre-mining background radiation levels in areas prone to future mine-dust pollution were required for future checks on any changes in background levels caused by uranium mining. Therefore, this study measured the pre-mining ambient dose equivalent rates due to background gamma radiation around a prospective uranium mine in the Manyoni District. The ambient dose equivalent, $H^*(10)$ in sievert units (Sv), is an operational quantity for area monitoring, and its rates have been determined in various studies to obtain the status of background radiation in the environment [8–11]. The results of this work are essential for assessing the future status of operational monitoring of uranium mining and the effectiveness of the decommissioning process in order to regulate environmental radioactive contamination.

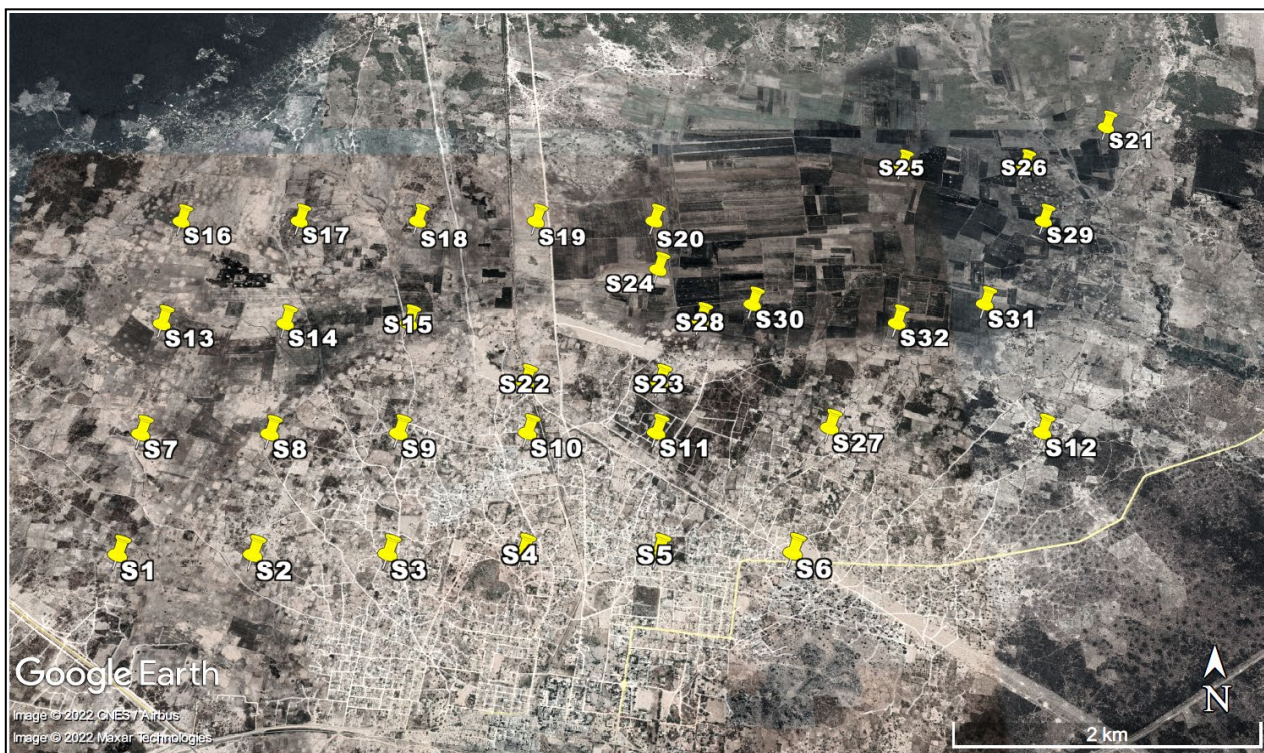
2. MATERIALS AND METHODS

2.1. The study area

The study area for this research is located between latitudes -5.694167° and -5.744167° and longitudes 34.796944° and 34.882500° in the Manyoni district of central Tanzania. The Manyoni district is home to the Manyoni Uranium Project, which contains up to 11,146 metric tonnes of uranium resources in surficial-type deposits [12]. The study area, which is also around the Manyoni Project area, was identified by dispersion modelling of anticipated mine dust using the American Meteorological Society-Environmental Protection Agency Regulatory Model (AERMOD), as detailed in Lolila et al. [13]. The modelling process took into account factors like weather, topography, and dust emission rates [13]. The sampling points chosen in the study area were determined by Lolila et al. [14] in two ways. In the first way, stratified sampling coupled with systematic sampling was used in a region expected to

receive mine-dust particles with mean annual ground level concentrations (AGLC) of PM₁₀ greater than or equal to 10% of the World Health Organisation (WHO) guideline limit of 20 µg/m³ [15]. In this way, 32 sampling points labelled S1–S32 were allocated to Site A, as shown in Figure 1. The 32 sampling points were in two different geological formations: the terrestrial coarse clastic sediments, laterite, and alterite, which made up 12.34% of the study area, and the gneiss-granite-migmatite complex, which made up 87.66% of the study area [14,16]. In the second way, judgmental sampling was used in an area expected to receive dust particles with mean AGLC of PM₁₀ greater than or equal to the WHO guideline limit of 20 µg/m³ [15]. In this way, 8 sampling points labelled H1–H8 were allocated at Site B, as shown in Figure 2. The 8 sampling points were within the same gneiss-granite-migmatite complex geology [14,16]. In both sites, measurements of ambient dose equivalent rates were determined, as detailed in the next section.

Figure 1: A map showing 32 sampling points, S1–S32, chosen for sampling at Site A



Source: Google Earth

2.2. Measurements of ambient dose equivalent rates

A Gamma-Scout portable radiation survey meter was used to measure ambient gamma dose equivalent rates in the air at 1 metre above the ground at forty (40) predetermined sampling points, shown in Figures 1 and 2, around the Manyoni uranium deposit. The survey meter was programmed to display a radiation dose rate reading every 2 seconds. According to the manufacturer's specifications, the survey meter was calibrated to measure radiation levels ranging from 0.01 $\mu\text{Sv/h}$ to 5,000 $\mu\text{Sv/h}$. To evaluate its performance, the survey meter was further calibrated against a ^{137}Cs standard source at the Tanzania Atomic Energy Commission's Secondary Standard Dosimetry Laboratory.

Figure 2: A map showing 8 sampling points, H1–H8, chosen for sampling at Site B



Source: Google Earth

Before taking measurements of the ambient dose equivalent rates (in $\mu\text{Sv/h}$) at a sampling point, the calibrated survey meter was held 1 m above the ground, turned on, and allowed to stabilise for 1 minute. After stabilisation, a dose rate at a sampling point was read and recorded every 5 seconds. To improve statistics, twenty (20) readings of the ambient dose equivalent rates were taken at a sampling point, five in each of the four cardinal directions (north, east, south, and west), and the average value

was determined to represent the ambient dose equivalent rate (in $\mu\text{Sv/h}$) at the sampling point. All measurements were taken outdoors during the day in February 2022. The measurement procedure explained above was performed for all 40 sampling points: 32 (S1–S32) selected in Site A, and 8 (H1–H8) selected in Site B (Figures 1 and 2).

3. RESULTS AND DISCUSSION

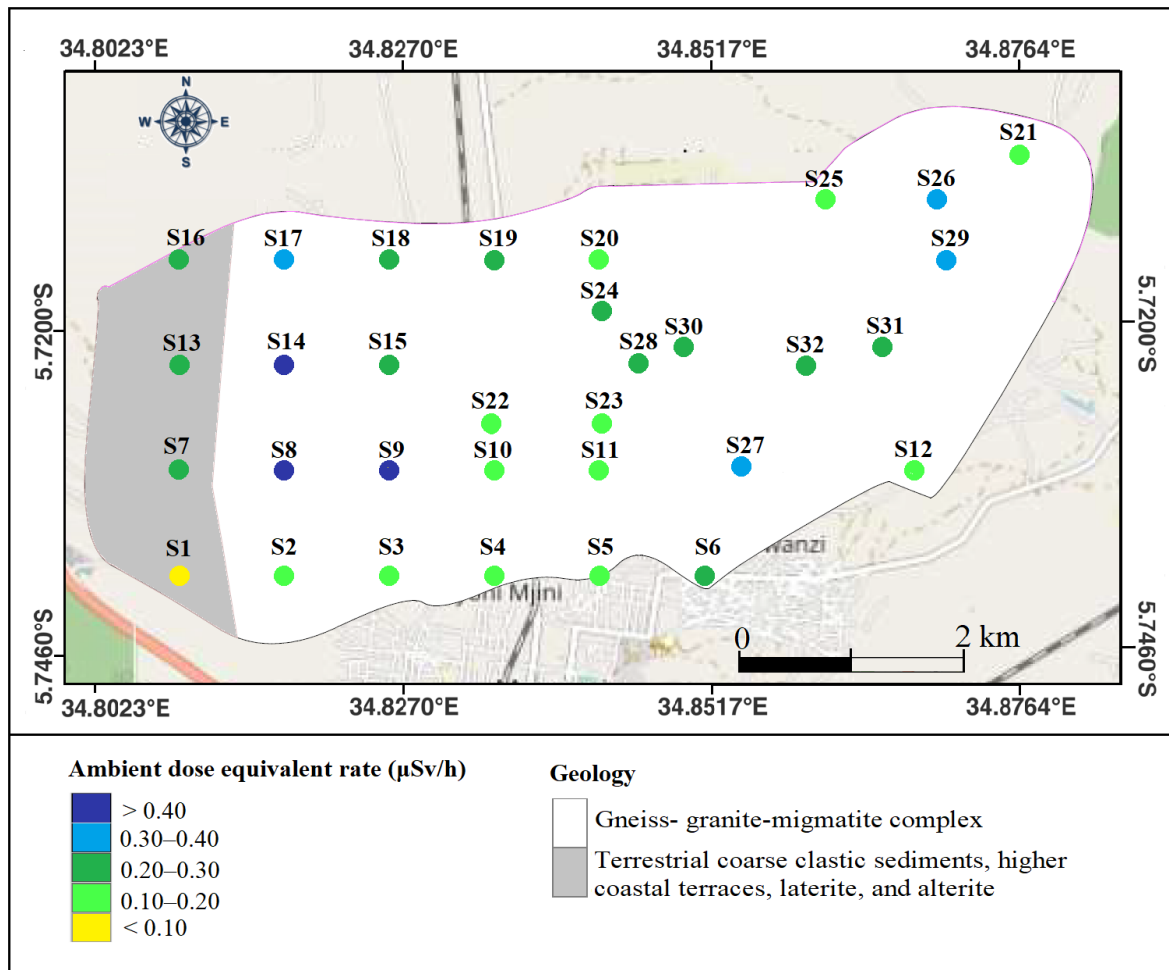
3.1. Ambient dose equivalent rate at Site A

The mean and ranges of the outdoor ambient dose equivalent rates measured at 1 m above the ground for the selected locations in Site A are presented in Table 1. The mean of ambient dose equivalent rates varied from 0.08 to 0.69 $\mu\text{Sv/h}$ with an overall average value of $0.25 \pm 0.03 \mu\text{Sv/h}$. It can be noted that the mean ambient dose rate was the highest at location S8 (0.69 $\mu\text{Sv/h}$) and the lowest at location S1 (0.08 $\mu\text{Sv/h}$) (Table 1). To illustrate the influence of geology on the spatial distribution of ambient dose equivalent rates, the mean dose rates for each sampling point were color-coded and superimposed on the geological map of the study area, as shown in Figure 3. From Figure 3 it can be noted that the ambient dose equivalent rates varied spatially, with relatively high values ($> 0.40 \mu\text{Sv/h}$) found at locations S8, S14, and S9 within the gneiss-granite-migmatite complex geology. The presence of radioactively rich granite in the gneiss-granite-migmatite complex geology may account for the observed high dose rates. In the same geology, a series with locations S15, S18, S19, S24, S28, S30, S32, and S31 had dose rates ranging from 0.20 to 0.30 $\mu\text{Sv/h}$. In addition, another series with locations S2, S3, S4, S5, S11, S23, S22, and S10 had dose rates ranging from 0.10 to 0.20 $\mu\text{Sv/h}$. Figure 3 also shows that location S1 in the terrestrial coarse clastic sediments, laterite, and alterite geology had the lowest dose rate ($< 0.10 \mu\text{Sv/h}$). In the same geology as S1, a series with locations S7, S13, and S16 had dose rates ranging from 0.20 to 0.30 $\mu\text{Sv/h}$.

Table 1: Ambient dose equivalent rates at Site A

Sampling point	Latitude	Longitude	Ambient dose equivalent rate ($\mu\text{Sv/h}$)	
			Range	Mean
S1	-5.737650°	34.808255°	0.06–0.09	0.08
S2	-5.737623°	34.816672°	0.13–0.17	0.14
S3	-5.737597°	34.825089°	0.09–0.12	0.11
S4	-5.737570°	34.833505°	0.11–0.20	0.14
S5	-5.737543°	34.841922°	0.09–0.22	0.14
S6	-5.737516°	34.850339°	0.17–0.24	0.21
S7	-5.729220°	34.808229°	0.24–0.33	0.28
S8	-5.729193°	34.816645°	0.66–0.71	0.69
S9	-5.729166°	34.825062°	0.52–0.68	0.60
S10	-5.729139°	34.833478°	0.11–0.16	0.13
S11	-5.729112°	34.841895°	0.18–0.20	0.19
S12	-5.729031°	34.867144°	0.15–0.20	0.18
S13	-5.720789°	34.808202°	0.22–0.29	0.24
S14	-5.720763°	34.816619°	0.42–0.67	0.61
S15	-5.720736°	34.825035°	0.19–0.22	0.21
S16	-5.712359°	34.808176°	0.21–0.34	0.27
S17	-5.712332°	34.816592°	0.29–0.35	0.32
S18	-5.712305°	34.825008°	0.21–0.22	0.21
S19	-5.712279°	34.833425°	0.20–0.23	0.21
S20	-5.712252°	34.841841°	0.14–0.23	0.18
S21	-5.703713°	34.875478°	0.15–0.25	0.19
S22	-5.725371°	34.833176°	0.15–0.19	0.17
S23	-5.725342°	34.842129°	0.16–0.19	0.18
S24	-5.716373°	34.842101°	0.18–0.25	0.22
S25	-5.707347°	34.859979°	0.16–0.21	0.18
S26	-5.707318°	34.868932°	0.36–0.43	0.39
S27	-5.728730°	34.853233°	0.31–0.35	0.34
S28	-5.720512°	34.844975°	0.24–0.29	0.27
S29	-5.712187°	34.869642°	0.26–0.33	0.31
S30	-5.719226°	34.848580°	0.20–0.24	0.22
S31	-5.719174°	34.864590°	0.13–0.45	0.23
S32	-5.720672°	34.858394°	0.22–0.32	0.26
Range			0.06–0.71	0.08–0.69
Average \pm Standard error			–	0.25 \pm 0.03

Figure 3: Ambient dose equivalent rates superimposed on the geological map of Site A



3.2. Ambient dose equivalent rate at Site B

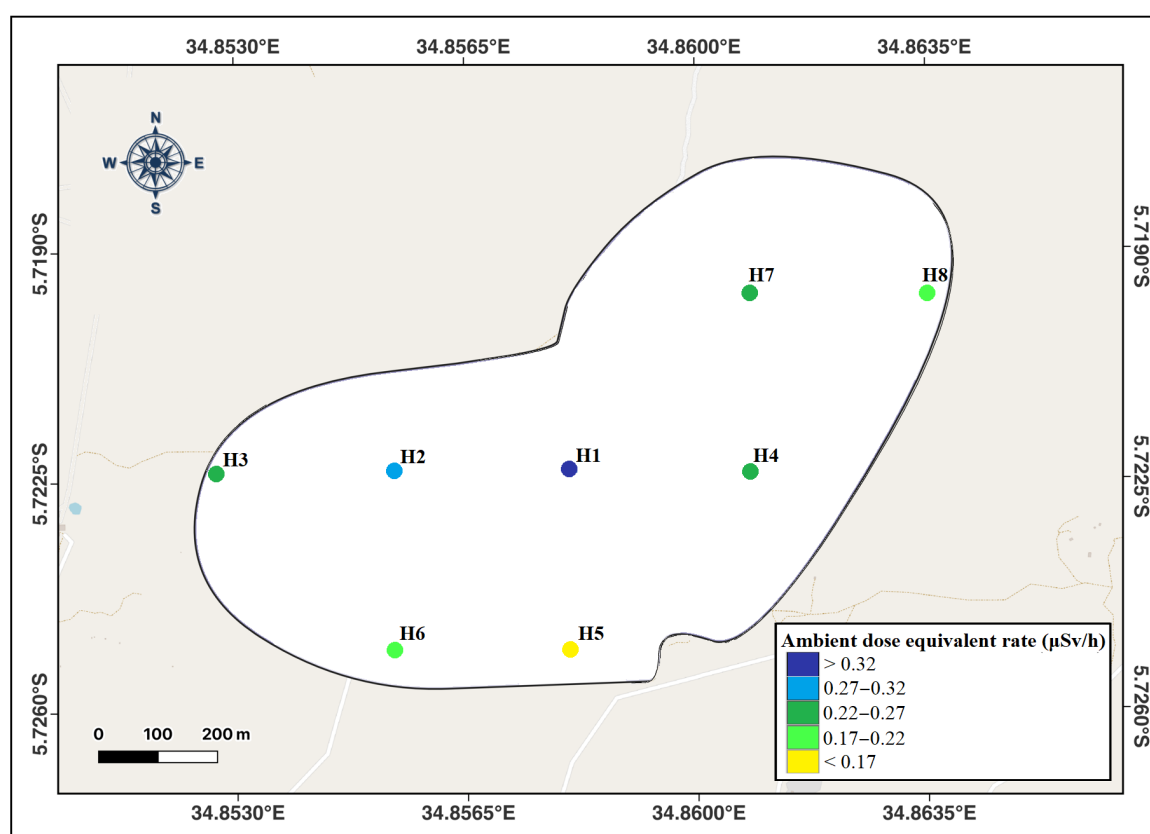
The results obtained from measurements of the ambient dose equivalent rates, due to gamma radiation, at locations H1–H8 at Site B are presented in Table 2. The mean ambient dose equivalent rates were found to be lowest in location H5 at $0.12 \mu\text{Sv/h}$ and highest in location H1 at $0.34 \mu\text{Sv/h}$, with an overall average value of $0.23 \pm 0.02 \mu\text{Sv/h}$. This average value is comparable to that found at Site A, which was $0.25 \pm 0.03 \mu\text{Sv/h}$.

The spatial distribution of ambient dose equivalent rates at Site B was also visualised by color-coding the dose rates on a map. Figure 4 shows that at Site B, which has the same gneiss-granite-migmatite complex geology, the ambient dose rates were spatially variable. Locations H1 and H2 had relatively high dose rates ($> 0.27 \mu\text{Sv/h}$), while H5 had the lowest dose rate ($< 0.17 \mu\text{Sv/h}$) (Figure 4).

Table 2: Ambient dose equivalent rates at Site B

Sampling point	Latitude	Longitude	Ambient dose equivalent rate ($\mu\text{Sv/h}$)	
			Range	Mean
H1	-5.719623°	34.857347°	0.30–0.37	0.34
H2	-5.719632°	34.854639°	0.22–0.33	0.28
H3	-5.719641°	34.851931°	0.16–0.29	0.23
H4	-5.719615°	34.860055°	0.19–0.31	0.24
H5	-5.722336°	34.857356°	0.11–0.13	0.12
H6	-5.722345°	34.854648°	0.16–0.20	0.18
H7	-5.716902°	34.860046°	0.23–0.29	0.26
H8	-5.716893°	34.862754°	0.13–0.25	0.19
Range			0.11–0.37	0.12–0.34
Average \pm Standard error			–	0.23 \pm 0.02

Figure 4: Distribution of ambient dose equivalent rates at Site B



3.3. Comparison with previous studies

Table 3 compares the ambient dose equivalent rates found in the vicinity of the Manyoni uranium deposit (this study) to those found in studies carried out in other countries. It is clear that Manyoni's average dose rates for sites A and B were comparable to the average dose rate that [8] discovered in southwestern Nigeria. Some similarities between the geology of southwestern Nigeria, which ranges from sandstones and clayey gravels to quartz and migmatite gneiss complexes [8], and the geology of Manyoni, which ranges from gneiss-granite-migmatite complex to coarse clastic sediments, laterite, and alterite, could be responsible for the observed similarity in average dose rates. On the other hand, the Manyoni's average dose rates for sites A and B were higher than those found in Najaf City (Iraq) [9], Metro Manila (Philippines) [10], and Iran [11]. The observed variations in average dose rates could be explained by geological differences between the study areas; however, those studies did not report comprehensive geological formations of their study areas.

Table 3: Comparison of ambient dose equivalent rates from different countries

Country	Study area	Ambient dose equivalent rate ($\mu\text{Sv/h}$)		Reference
Tanzania	Manyoni (at Site A)	Mean Range	0.25 0.08–0.69	This study
Tanzania	Manyoni (at Site B)	Mean Range	0.23 0.12–0.34	This study
Nigeria	Southwestern Nigeria	Mean Range	0.21 0.06–0.52	[8]
Iraq	Najaf city	Mean Range	0.08 0.06–0.12	[9]
Philippines	Metro Manila	Mean Range	0.04 0.03–0.06	[10]
Iran	Iran	Mean Range	0.063 0.005–0.164	[11]

4. CONCLUSION

This study established pre-mining ambient gamma dose equivalent rates around a prospective uranium mine in the Manyoni District. The ambient dose equivalent rates were measured at two sites, A and B, that are expected to be affected by mine-dust (PM₁₀) pollution as a result of future uranium mining activities. It was found that the average of the ambient dose equivalent rates was 0.25 ± 0.03 $\mu\text{Sv/h}$ at Site A with 32 sampling points and 0.23 ± 0.02 $\mu\text{Sv/h}$ at Site B with 8 sampling points. The mean ambient equivalent dose rates for each sampling point were also presented. The effect of local geology on measured dose rates was also demonstrated by superimposing dose rate plots on the geological map of the study area. The information presented in this study can be used as a baseline for monitoring potential contamination in the future when uranium mining commences. It can also be used as a guide for future surveys of ambient gamma dose equivalent rates around the Manyoni uranium deposit or other places with uranium deposits.

ACKNOWLEDGMENT

The authors would like to thank the Dar es Salaam University College of Education for funding this research.

REFERENCES

- [1] UNSCEAR - United Nations Scientific Committee on the Effects of Atomic Radiation. **Sources and effects of ionizing radiation: United Nations Scientific Committee on the Effects of Atomic Radiation: UNSCEAR 2000 report to the General Assembly, with scientific annexes. Volume I: Sources.** New York: United Nations, 2000.
- [2] BAI, H.; HU, B.; WANG, C.; BAO, S.; SAI, G.; XU, X.; ZHANG, S.; LI, Y. Assessment of radioactive materials and heavy metals in the surface soil around the Bayanwula prospective uranium mining area in China. **Int J Environ Res Public Health**, v. 14, article 300, 2017.

- [3] BANZI, F. P.; MSAKI, P. K.; MOHAMMED, N. K. Assessment of natural radioactivity in soil and its contribution to population exposure in the vicinity of Mkuju River uranium project in Tanzania. **Expert Opin Environ Biol**, v. 6, article 140, 2017.
- [4] SEMIONO, P.; MWALONGO, D. A.; MKILAHA, I. S. N.; MATO, R. R. A. M.; JACKSON, M. M. Investigation of natural background gamma ray doses in the proposed uranium mines at Bahi and Manyoni. **Ethiop J Environ Stud Manag**, v. 10, p. 1094–1105, 2017.
- [5] TOP, G.; ÖRGÜN, Y.; AYAZLI, I. E.; BELIVERMIS, M.; KARACIK, Z.; KAMPFL, G. Determination of Ra-226, Th-232, K-40 and Cs-137 activities in soils and beach sands and related external gamma doses in Arikli mineralization area (Ayvacik/Turkey). **Radiat Prot Dosimetry**, v. 193, p. 137–154, 2021.
- [6] MAJAWA, L. J.; TSHIVHASE, V. M.; DLAMINI, T. Radioactivity assessment of surface soil in the vicinity of a uranium mine in Malawi. **Radiat Prot Dosimetry**, v. 198, p. 1353–1360, 2022.
- [7] LOLILA, F.; MAZUNGA, M. S. Measurements of natural radioactivity and evaluation of radiation hazard indices in soils around the Manyoni uranium deposit in Tanzania, **J Radiat Res Appl Sci**, v. 16, article 100524, 2023.
- [8] OKEYODE, I. C.; RABIU, J. A.; ALATISE, O. O.; MAKINDE, V.; AKINBORO, F. G.; AL-AZMI, D.; MUSTAPHA, A. O. Area monitoring of ambient dose rates in parts of south-western Nigeria using a GPS-integrated radiation survey meter. **Radiat Prot Dosimetry**, v. 173, p. 263–267, 2017.
- [9] LAITH, S. Background Radiation in Najaf city, Iraq. **World Sci News**, v. 92, p. 378–384, 2018.
- [10] ENCABO, R. R.; CRUZ, P. T. F.; BONGA, A. C.; DELA SADA, C. L.; OMANDAM, V. J.; OLIVARES, J. U.; IWAOKA, K.; FELICIANO, C. P. Measurement of ambient gamma dose rate in Metro Manila, Philippines, using a portable NaI(Tl) scintillation survey meter. **Environ Monit Assess**, v. 192, article 400, 2020.
- [11] KARDAN, M. R.; SADEGHI, N.; FATHABADI, N.; ATTARILAR, A. Assessment of terrestrial radiation by direct measurement of ambient dose equivalent rate of background radiation. **Radiat Prot Dosimetry**, v. 184, p. 189–197, 2019.
- [12] Nuclear Energy Agency; International Atomic Energy Agency. **Uranium 2016: resources, production and demand**. Paris: OECD Publishing, 2016.

- [13] LOLILA, F.; MAZUNGA, M. S.; NDABENI, N. B. Demarcation of pollution-prone areas around the Manyoni Uranium Project, Tanzania. **Aerosol Air Qual Res**, v. 22, article 220214, 2022.
- [14] LOLILA, F.; MAZUNGA, M.; NDABENI, N. Baseline measurements of natural radioactivity around the Manyoni uranium deposit (Tanzania): selection of sampling points. **Menemui Matematik**, v. 44, p. 97-108, 2022.
- [15] WHO - World Health Organisation. **Air quality guidelines: global update 2005: particulate matter, ozone, nitrogen dioxide and sulfur dioxide**. Copenhagen: WHO Regional Office for Europe, 2006.
- [16] GEOLOGICAL SURVEY OF TANZANIA. **Geological and Mineral Information System**. n.d. Available at: <<https://www.gmis-tanzania.com/>>. Last accessed: 29 March 2023.

This article is licensed under a Creative Commons Attribution 4.0 International License, which permits use, sharing, adaptation, distribution and reproduction in any medium or format, as long as you give appropriate credit to the original author(s) and the source, provide a link to the Creative Commons license, and indicate if changes were made. The images or other third-party material in this article are included in the article's Creative Commons license, unless indicated otherwise in a credit line to the material.

To view a copy of this license, visit <http://creativecommons.org/licenses/by/4.0/>.